Supporting Information:
Reef fish functional groups show variable declines due to deforestation-driven sedimentation, while flexible harvesting mitigates this damage

Russell Milne[1,2,*,†], Madhur Anand[1,2], Chris T. Bauch[1,2]

1 Department of Applied Mathematics, University of Waterloo, Waterloo, Ontario, Canada
2 School of Environmental Sciences, University of Guelph, Guelph, Ontario, Canada

* Corresponding author. Email address: r2milne@uwaterloo.ca
† Current address: Department of Mathematical and Statistical Sciences, University of Alberta, Edmonton, Alberta, Canada

A Model construction

A.1 Fish trophic interactions

Since turf algae and macroalgae were assumed to be grazed at rates $g_{_T}$ and $g_{_M} \leq g_{_T}$, respectively, it can be further assumed that the relative proportions of turf algae and macroalgae consumed by grazers (such as herbivorous fish) can be represented with the ratio $\frac{g_{_M}}{g_{_T}} \leq 1$. Hence, we took $T + \frac{g_{_M}}{g_{_T}} M \leq 1$ as the scaling term for herbivorous fish growth. As rates of herbivory are negatively impacted by accumulation of algal turf sediment [1, 2], we introduced another quantity $\mu(t)$ representing this decrease. $\mu(t)$ depends on sediment quantities on the seabed, and is further explained below. We assumed that herbivorous fish would be eaten by piscivorous fish and top predators, with $\delta_{_P}$ denoting the percentage of the diet of piscivores made up by herbivores and $\delta_{_Z}^{H}$ denoting this percentage for top predators. This meant that our scaling constant for herbivorous fish predation was taken to be $\frac{\delta_{_P} F_{_P} + \delta_{_Z}^{H} F_{_Z}}{\delta_{_P} + \delta_{_Z}^{H}} \leq 1$. Therefore, after also accounting for the harvesting term $-h_{_H} F_{_H}$, we represented the differential equation for herbivorous fish as follows:

$$\frac{\mathrm{d}F_{_H}}{\mathrm{d}t} = \frac{r_{_H}}{1+\mu} F_{_H} \left(1 - F_{_H}\right) \left(T + \frac{g_{_M}}{g_{_T}} M\right) - h_{_H} F_{_H} - m_{_H} F_{_H} \frac{\delta_{_P} F_{_P} + \delta_{_Z}^{H} F_{_Z}}{\delta_{_P} + \delta_{_Z}^{H}} \tag{A.1}$$

The diet of omnivorous fish typically consists partly of primary producers (e.g. algae) and partly of other food sources such as zooplankton and small invertebrates [3]. We defined $\delta_{_O}$ as the percentage of an omnivorous fish's diet consisting of algae, and assumed that omnivorous fish would consume turf algae and macroalgae at the same relative rates as herbivorous fish. This was scaled down by μ in the same way as in the dynamics for herbivorous fish. This implies that $(1 - \delta_{_O})$ percent of an onmivorous fish's diet consists of other food sources, the availability of which we modelled using a function $\phi(t)$ (see below). As with herbivorous fish, we assumed that omnivorous fish were eaten by piscivorous fish (composing $(1 - \delta_{_P})$ percent of their diet) and top predators (composing $\delta_{_Z}^{O}$ percent of their diet), and harvested at a constant rate. Therefore, the dynamics of omnivorous fish are represented as follows:

$$\frac{\mathrm{d}F_{O}}{\mathrm{d}t} = r_{O}F_{O}\left(1-F_{O}\right)\left(\frac{\delta_{O}}{1+\mu}\left(T+\frac{g_{M}}{g_{T}}M\right)+\left(1-\delta_{O}\right)\phi\right) - h_{O}F_{O} - m_{O}F_{O}\frac{(1-\delta_{P})F_{P}+\delta_{Z}^{O}F_{Z}}{1-\delta_{P}+\delta_{Z}^{O}} \tag{A.2}$$

As detailed above, piscivorous fish were assumed to eat both herbivorous and omnivorous fish, in proportions δ_{P} and $(1-\delta_{P})$, respectively. They are, in turn, eaten by top predators and harvested. Note that the proportion of top predator diet that piscivorous fish make up is $1-\delta_{Z}^{H}-\delta_{Z}^{O}$. As the total predation pressure on piscivorous fish is therefore $F_{Z}\left(1-\delta_{Z}^{H}-\delta_{Z}^{O}\right)$, but scaling this to values between 0 and 1 involves dividing by $1-\delta_{Z}^{H}-\delta_{Z}^{O}$, this constant is normalized out of the differential equation governing piscivorous fish dynamics. The differential equation in question is as follows:

$$\frac{\mathrm{d}F_{P}}{\mathrm{d}t} = r_{P}F_{P}\left(1-F_{P}\right)\left(\delta_{P}F_{H}+\left(1-\delta_{P}\right)F_{O}\right) - h_{P}F_{P} - m_{P}F_{P}F_{Z} \tag{A.3}$$

Top predators consume fish from all other functional groups, according to the proportions mentioned above. As they lack predators by definition, the sources of their mortality are assumed to be harvesting and natural causes. This yields the following differential equation for top predators:

$$\frac{\mathrm{d}F_{Z}}{\mathrm{d}t} = r_{Z}F_{Z}\left(1-F_{Z}\right)\left(\delta_{Z}^{H}F_{H}+\delta_{Z}^{O}F_{O}+\left(1-\delta_{Z}^{H}-\delta_{Z}^{O}\right)F_{P}\right) - h_{Z}F_{Z} \tag{A.4}$$

Fung *et al.* did not explicitly include grazer populations in their model, and hence represented grazing pressure as a constant θ. We instead use a baseline rate $\tilde{\theta}$ scaled by the population levels of herbivorous and omnivorous fish relative to their theoretical maxima, with the contribution of omnivorous fish to grazing being the proportion of their diet consisting of algae. The grazing rate also decreases as sediment levels increase, so we additionally divide by $1+\mu$ (as in the grazing terms of F_{H} and F_{O}) to represent this. Specifically, we take θ to be the following:

$$\theta(t) = \frac{\tilde{\theta}\left(F_{H}+\delta_{O}F_{O}\right)}{\left(1+\mu\right)\left(1+\delta_{O}\right)} \tag{A.5}$$

A.2 Deforestation and sediment dynamics

Changes in forest cover were modelled in a variety of different ways, to represent unmanaged deforestation and managed logging. For our baseline scenario, we assumed a steady loss of forest cover scaling with population increases. Here, we drew on the work of Tanaka and Nishii [4] which modelled the percentage change in forest cover per unit change in area population; we defined r_{X} as the linear rate of deforestation referred to as r in [4]. We obtained values for population N and population change $\frac{\mathrm{d}N}{\mathrm{d}t}$ based on the medium-variant United Nations projections for tropical island states in Oceania [5], specifically the Sustainable Development Goals region of Oceania (excluding Australia and New Zealand). We also assumed a background rate of forest regrowth, governed by the rate a_{X}. We took the forest regrowth term to be logistic, as the rate of forest expansion into cleared land should decrease as the amount of available cleared land does; we assumed a carrying capacity of 1, or 100% forest cover. Therefore, the differential equation for forest cover, $\frac{\mathrm{d}X}{\mathrm{d}t}$, was taken to be the following:

$$\frac{\mathrm{d}X}{\mathrm{d}t} = \frac{\mathrm{d}X}{\mathrm{d}N}\frac{\mathrm{d}N}{\mathrm{d}t} + a_{X}X(1-X) = -r_{X}NX\frac{\mathrm{d}N}{\mathrm{d}t} + a_{X}X(1-X) \tag{A.6}$$

Sediment export onto reefs was assumed to change due to deforestation, and specifically increase due to increased erosion when forest cover was low. The amount of sediment being deposited onto reefs due to soil erosion typically increases linearly as forest cover is reduced [6, 7]. We took q_b to be the baseline river sediment concentration at 100 percent forest cover, and q_c to represent the additional amount of sediment in rivers when all land has been cleared; both of these have units of mg cm^{-3}. We also took λ (measured in yr^{-1}) as the rate at which sediment in these rivers is exported into the water column. Once sediment is suspended in the water column above a reef, it can be washed out further into the ocean or settle on the seabed. We took e to be the rate at which sediment is washed out of a reef ecosystem, and assumed that the amount of sediment on the seabed would be in equilibrium with the amount suspended in the water column. The differential equation for S_W is therefore as follows:

$$\frac{\mathrm{d}S_W}{\mathrm{d}t} = \left(q_b + (1 - X)\, q_c\right) \lambda - e S_W \tag{A.7}$$

Here, the term eS_W covers both initial export of sediment by rivers to areas beyond a reef (which first must physically pass through the reef area) and later off-shelf export of sediment in the water above a reef. This was done since both of these processes are significant [8, 9] and data that could be used to separate the two was not readily available. Because suspended sediment and sediment on the seabed are measured in different units (mass per unit volume and per unit area, respectively), and converting between these may be difficult, we opted to express sediment on the seabed as a ratio between the level at any given time and levels corresponding to pristine conditions. A corollary of our assumption that accumulated seabed sediment is in equilibrium with suspended sediment concentration is that the growth in these two variables is proportional to each other, and expressing S_B as a ratio (i.e. indexing a value of $S_B = 1$ to pristine conditions) rather than as a differential equation eliminates the need for a growth rate constant. We therefore took S_B to be the following:

$$S_B\left(t\right) = \frac{S_W\left(t\right)}{S_W\left(t = 0\right)} \tag{A.8}$$

Fung *et al.* identified sedimentation as affecting four processes in their model, namely lateral coral growth (described using r_C), larval recruitment of both local brooding and exogenous spawning corals (l_C^b and l_C^s, respectively), and coral death (d_C). The existing literature describes changes in these processes as functions of sedimentation rates, rather than the total amount of sediment either in the water column or on the seabed (see e.g. [10] Appendix B). We therefore assumed that these processes could be described as baseline rates $\tilde{r}_C$, $\tilde{l}_C^b$, $\tilde{l}_C^s$, and $\tilde{d}_C$ scaled up or down according to the sedimentation rate. Much of the redistribution of sediment on reefs is performed by parrotfish [11, 12], which bite into sediment while feeding and therefore reduce sediment buildup on reefs, lowering the effective sedimentation rate, although other herbivorous fish with different feeding methods also may have effects on sediment accumulation [12]. In a recent experiment in which areas of seabed were caged off to simulate a herbivorous fish density of zero, Akita *et al.* found that the caged areas had on average double the accumulated sediment levels compared to uncaged control sites [13]. All of the control sites in [13] were fished, and herbivorous fish landings in the area were reported as being half of what was caught in the 1990s, suggesting that herbivorous fish density there would be at most half of its theoretical maximum. Since the sedimentation rates (mass per unit area per unit time) observed by [13] were similar to pristine values observed elsewhere (see below), we therefore assumed that the sedimentation rate would begin linearly increasing when the

herbivorous fish population declined below a value of 0.5, and would double when no herbivorous fish were present. Hence, we defined the sedimentation rate as follows:

$$r_{\text{Sed}} = \max[1 + (1 - 2H), 1]\, k_{\text{Dep}} S_W \tag{A.9}$$

This formulation uses a constant k_{Dep} to represent the baseline rate of sediment deposition, as well as incorporating dependence on the population of herbivorous fish. (We took k_{Dep} to have units of $100 \times$ cm yr^{-1}. This is done so that the rate of sedimentation is expressed over an area rather than a volume, and hence can be calibrated to observed field values that are measured in mg cm^{-2} time^{-1}. The scaling down of k_{Dep} by a factor of 100 was done because the field data on sedimentation rates that we fit our model to had time units of days, while time in our model is expressed in years, and we intended to keep our sedimentation rate on the same order of magnitude as the raw numbers seen in the field.) Because the three coral growth processes were negatively affected by sedimentation, we modelled them as follows:

$$r_C(t) = \frac{\tilde{r}_C \kappa_r}{\kappa_r + r_{\text{Sed}}}; \quad l_C^b(t) = \frac{\tilde{l}_C^b \kappa_b}{\kappa_b + r_{\text{Sed}}}; \quad l_C^s(t) = \frac{\tilde{l}_C^s \kappa_s}{\kappa_s + r_{\text{Sed}}} \tag{A.10}$$

Here, κ_r, κ_b, and κ_s are constants that determine at which sedimentation rate the corresponding coral growth rate is halved. Coral death instead increases when sedimentation rate is high. This means that the sedimentation-dependent coral death rate can be taken as the following, with κ_d a scaling constant:

$$d_C(t) = \tilde{d}_C \left(1 + \frac{r_{\text{Sed}}}{\kappa_d}\right) \tag{A.11}$$

In addition to sedimentation's effects on coral, the buildup of algal turf sediment (i.e. sediment on the seabed contained under and within areas dominated by algal turf) is known to inhibit herbivory of algae [1, 2]. As mentioned above, we modelled this by using a factor μ to divide the rates of grazing and herbivory in the model. We assume here that sediment is evenly distributed on the seabed, so the amount of sediment accumulated there is a good proxy for algal turf sediment, and hence the extent to which local algal turf is closer to being SPAT (short, productive algal turf, the kind preferred by herbivorous fish) or LSAT. This can be done because the correlation between seabed sediment load and algal turf length is roughly linear [2]. Tebbett *et al.* found that approximately doubling seabed sediment concentration from pristine values led to herbivorous fish bites on algae approximately halving, and a quadrupling of sediment concentration led to a 78% reduction in herbivorous fish bites compared to the pristine baseline (i.e. approximately another halving from the value with doubled sediment levels) [2]. Similarly, it has been found that removal of large amounts of sediment from reef flats (where seabed sediment buildup is greater) had similar effects on encouraging herbivory as removing much smaller amounts of sediment from reef areas with less sediment buildup [1], indicating the sensitivity of herbivorous fish to algal turf sediment levels. Because of this, we assumed that μ would increase logarithmically with the amount of sediment on the seabed, with a logarithm base of 2 due to the repeated halvings mentioned above. This means that our formulation for μ is as follows:

$$\mu = \max[\log_2(S_B), 0] \tag{A.12}$$

Much of the diet of omnivorous fish consists of zooplankton [3]. The phytoplankton that zooplankton eat can have their population growth limited by low light availability, such as in turbid

waters, making planktonic food webs vulnerable to suspended sediment increases [14]. Zooplankton dynamics (and hence zooplankton-phytoplankton trophic interactions) happen over a faster timescale than the rest of the processes in our model [15], and plankton population dynamics are also less complex in more active waters [16] such as those near the mouth of a river. Therefore, we assumed a direct dependence of $\phi(t)$ on suspended sediment concentration. This involved scaling ϕ with light availability according to the Lambert-Beer law [17], which is the following function relating underwater light intensity I to intensity of the light source I_0, depth d, and light attenuation constant k_{att}:

$$I = I_0 e^{-k_{\text{att}} d} \tag{A.13}$$

We took the light attenuation constant k_{att} to vary based on suspended sediment concentration. A linear relationship has been found between these two quantities in estuarine waters [18], which has a slope of 60 when suspended sediments are measured in mg cm^{-3}. Furthermore, we assumed that $\phi = 1$ in pristine conditions (to bound the growth rate of omnivorous fish above by 1), and that water depth was constant. These constraints meant that we took the following form for ϕ:

$$\phi = \exp\Big(-\tilde{\phi} S_W\Big); \quad \tilde{\phi} = 60 \tag{A.14}$$

Algae on the seabed also undergoes photosynthesis, and coral obtains much of its energy from dinoflagellate symbionts, which in turn get their energy from photosynthesis. However, the reduction in coral growth and reproduction rates due to sedimentation (including from photosynthesis reduction) is already included in the model via processes detailed by Fung *et al.* (see above). Additionally, Fung *et al.* considered reduction in algal photosynthesis due to sedimentation, but did not include it in their model due to lack of data. We also opted not to include this. Turf algae spread very rapidly, and have been found to dominate the benthos under conditions featuring high turbidity [19] or sedimentation rates [20, 21] due to their ability to trap sediment. Therefore, we assumed that although light attenuation due to turbidity may affect the growth of turf algae, it would not appreciably affect their spread if a reasonable amount of light still reached the seabed. Conversely, the steady-state macroalgae levels reached with our baseline parameter values were low enough that any difference due to decreasing photosynthesis would be minimal.

B Model parametrization

All parameters relating to transitions on the seabed between coral, macroalgae, turf algae and space that were used by Fung *et al.* were kept at the values specified in [10]. This includes the baseline values $\tilde{\theta}$, $\tilde{r}_C$, $\tilde{l}^b_C$, $\tilde{l}^s_C$, and $\tilde{d}_C$ for rates affected by features that we added to the model.

To keep our model applicable to a potentially broad range of reef areas experiencing deforestation, we chose the fish growth rates and diet composition ratios in our model based on observed properties of marine food webs rather than fitting them for fish in a specific region. Since generation time (and hence population growth rate) among aquatic species is negatively correlated with trophic level [22], we selected growth rates satisfying $r_H > r_O > r_P > r_Z$. Pristine reef areas typically have around 50 percent coral cover [23], which is not edible by herbivorous fish. We therefore chose $r_H = 1.6$, $r_O = 1.3$, $r_P = 1$, and $r_Z = 0.7$; our growth rate for herbivorous fish allows their population to double in approximately one year, as has been observed for many herbivorous reef fish species [3], when 50 percent of the benthos is available for them to eat.

As marine food webs, including those on coral reefs, have been found to have short average path lengths and considerable numbers of interspecies links [24], we assumed a relatively highly-clustered food web in which the diet of each predatory functional group would have significant contributions from each functional group that it preys on. Hence, we assumed that omnivorous fish ate algae and non-algal food sources (e.g. benthic invertebrates) at equal rates, i.e. $\delta_{O} = 0.5$. Similarly, we took the values of the top predator diet parameters to be $\delta_{Z}^{H} = 0.1$ and $\delta_{Z}^{O} = 0.3$ based on the assumption that top predators would eat more fish in higher trophic levels, and we took $\delta_{P} = 0.4$ for the same reason. However, in recognition of the fact that significant localized variation can exist in fish diet composition, we checked our model's output for values of $\pm 10\%$ in each diet composition constant. Specifically, we took each of δ_{O}, δ_{P}, δ_{Z}^{H}, and δ_{Z}^{O} to be 90%, 100%, and 110% of the values specified above (a total of 81 combinations of values) under the assumption of highland deforestation conditions, when all other parameters were at their baseline values. This did not cause noticeable qualitative differences in the time series for the fish functional groups over our 50-year simulation window, and had minimal effects on F_{H} and F_{O}, leading us to conclude that our model was robust to variation in the diet composition constants.

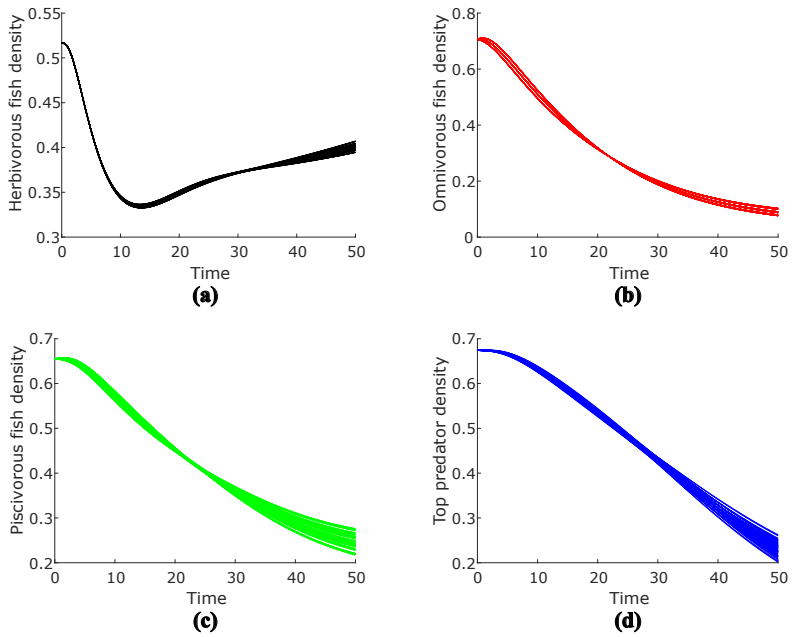

Figure B.1: Time series of herbivorous fish (Figure B.1a), omnivorous fish (Figure B.1b), piscivorous fish (Figure B.1c), and top predators (Figure B.1d) when each of the diet composition constants (δ_{O}, δ_{P}, δ_{Z}^{H}, and δ_{Z}^{O}) were varied by $\pm 10\%$.

Previous modelling studies have found a harvesting rate of 0.3 yr^{-1} to be close to the maximum rate at which fish populations can maintain themselves [25, 26]. In contrast, harvesting rates associated with subsistence fishing are typically an order of magnitude lower than those characteristic of commercial fishing [27]. We therefore assumed a baseline harvesting rate of 0.15 yr^{-1} for each functional group to represent the midpoint of plausible commercial rates, in the same way that the

midpoints of the seabed parameter ranges identified by Fung *et al.* were used as baseline values both by us and in Fung *et al.*'s original study. Where applicable, this was altered by the consideration of flexible harvesting rates, constant fishing quotas, and increased fishing pressure due to population growth; see below for details.

Sediment export onto reefs due to erosion is low in heavily forested areas, and increases with the proportion of cleared land [6, 7]. A recent survey on Isabel Island in the Solomon Islands found that over a catchment covered almost entirely by forest, sediment concentrations at the mouth of a local river (the Jejevo) had a geometric mean of 20 mg L^{-1}, or 0.02 mg cm^{-3} [28]. Since the waters at the mouth of the Jejevo have been found to be on average 15 times more turbid than those by adjacent rivers [29], we took q_b to have a high value of 0.02 mg cm^{-3} and a low value of 0.0013 mg cm^{-3}. In the wet tropics of northern Queensland, Australia, Neil *et al.* found a linear relationship between percentage of land cleared and suspended sediment concentration in local rivers during the wet seasons of specific years [6], thus controlling for temporal variation due to any ongoing changes in land use. Plugging 100 percent land clearance into the formulas in [6] yielded values of 72 and 14 mg L^{-1} for very wet and fairly wet conditions, respectively. Wenger *et al.* performed a similar analysis on Kolombangara Island in the Solomon Islands, based on future predictions of yearly erosion with varying percentages of cleared land [7]. That study found average suspended sediment concentration in streams to be 124 mg L^{-1} at 40 percent cleared land with no management, as well as a linear rate of increase for sediments, implying a concentration of 310 mg L^{-1} when land is fully cleared. The concentration at 100 percent forest cover found by Wenger *et al.* was similar to that found by Neil *et al.*; the difference in slope of the two relationships can be attributed to the fact that Wenger *et al.* considered deforestation on steeper terrain. We therefore took q_c to be 0.31 mg cm^{-3} when simulating deforestation on steep terrain, and 0.043 mg cm^{-3} (the average of the two values found by Neil *et al.*) for gentler terrain. This represents the increase in sedimentation due to erosion that an entirely cleared environment has compared to an entirely forested one.

Rates of sediment export from coastal into off-shelf areas have a great deal of spatial variation (see [8] for an example of this in New Guinea, with both very high and very low amounts of off-shelf export observed). Therefore, we took e to vary over a wide range, namely from 0.1 to 0.9, with the median value 0.5 used as a baseline. We assumed λ to be 1 yr^{-1} in order to simulate conditions on reefs near river mouths. Reefs further away can receive substantially less sediment from river discharges [30]; this process was folded into e in order to simplify the model analysis (see above), as e and λ perform similar functions (limiting sediment on reefs due to local hydrodynamics).

To find a value of k_{Dep}, we related suspended sediment concentrations to rates of sedimentation in a dataset covering Isabel Island [29], using the formula $r_{\text{Sed}} \approx k_{\text{Dep}} S_W$ in the absence of data on parrotfish abundance. We used the average reported turbidity in nephelometric turbidity units (NTUs) at the Jihro inshore reef site in that dataset, which was similar to those on other inshore reefs globally [29] such as on the Great Barrier Reef [12], to estimate suspended sediment concentration. A value in mg L^{-1} was obtained from this using a linear method used in [31], taking the average slope of 18 linear functions linking NTUs to sediment density, and this was further scaled to units of mg cm^{-3}. We then divided the observed sedimentation rates on inshore reefs in this dataset by the obtained average sediment concentration. This gave us an average value of 4400 for k_{Dep}, after disregarding an outlier, which had a sedimentation rate over 20 times higher than the other sites and was therefore deemed non-representative.

While parametrizing their model, Fung *et al.* estimated from field data that a sedimentation rate of 100 mg cm^{-2} d^{-1}, or 365×10^2 mg cm^{-2} yr^{-1}, causes coral lateral growth rate to decline by half (see [10] Appendix B). Hence, we took $\kappa_r = 365$. Similar estimates by Fung *et al.* included that

a sedimentation rate of 12 cm^{-2} d^{-1} causes larval recruitment of both brooding and spawning corals to decrease by 60%, and one of 13 cm^{-2} d^{-1} causes coral death rate to double. After converting units, this leads to a value of $\frac{44}{1.5}$ for $\kappa_{_b}$ and $\kappa_{_s}$, and a value of 47.5 for $\kappa_{_d}$.

We determined values for $r_{_X}$ by isolating it within the differential equation proposed by Tanaka *et al.* [4], i.e. $\frac{\text{d}F}{\text{d}N} = -r_{_X} F N$. To do this, we used data on deforestation in the Indonesian part of the island of Borneo (i.e. Kalimantan) from 1973 to 2000 and from 2000 to 2010 [32], and population growth data in Kalimantan over the same years [33]. For each of these time periods, we took F to be the percentage forest cover in Kalimantan at the end of the period and N to be the population of Kalimantan at the end of the period relative to its population at the beginning of the period, and estimated $\frac{\text{d}F}{\text{d}N}$ by dividing the change in forest cover by the relative change in population during the period. (2000 and 2010 were census years in Indonesia, and we estimated the 1973 population by assuming a linear rate of growth between the 1971 and 1980 censuses.) We used relative rates rather than absolute population numbers (as was done by Tanaka *et al.*) in order to control for population density and hence maximize applicability to different locations. From these calculations, we obtained a value of 0.18 for $r_{_X}$ from 1973 to 2000, and a value of 0.23 from 2000 to 2010. We therefore took 0.23 as a baseline for $r_{_X}$, although we allowed it to vary in order to simulate a variety of deforestation speeds.

A long-term study (from 1990 to 2020) on changes in forest cover in the tropics found that out of the undisturbed forest in insular Southeast Asia in 1990, 16.4 percent had been deforested, and 3.7 percent had been deforested and subsequently regrew [34]. This gives an estimate that the speed of reforestation was 0.18 times the speed of deforestation in this time period. Hence, we assumed our background rate of forest regrowth $a_{_X}$ to be 0.18 times the baseline value for $r_{_X}$ of 0.23, or in other words $a_{_X} \approx 0.04$.

In all model simulations that were performed in the generation of our results, the initial conditions for the model's state variables were chosen to be the equilibrium values reached when running the model with no deforestation (i.e. $X(t=0) = 1$, $r_{_X} = a_{_X} = 0$) but all other parameters at their baseline values. This was done to represent a viable reef ecosystem with sustainable harvesting of reef fish. The initial conditons that we chose are specified in Table B.3. To verify the effectiveness of this method for generating initial conditions, we checked the model for bistability when all parameters were taken as above. We found that nearly all combinations of initial conditions for all relevant state variables in our model (those besides X) resulted in convergence to the same equilibrium that we chose for our initial conditions, although very small values of $S(t=0)$ caused the model to converge to alternate attractors.

C Derivations of flexible harvesting rates

To evaluate the impact of flexible harvesting, we derived a harvesting rate that would change for each functional group based on local availability of fish in that functional group, while the percentage of the total fish population being harvested would remain constant. We first estimated the rate for all functional groups combined by taking a weighted average of the rates $h_{_H}$, $h_{_O}$, $h_{_P}$ and $h_{_Z}$, where the weights were set equal to the relative abundances of each functional group in the initial conditions we specified above. In other words, we defined the aggregate harvesting rate as follows:

$$h_{_{\text{Tot}}} = \frac{h_{_H} F_{_H}(0) + h_{_O} F_{_O}(0) + h_{_P} F_{_P}(0) + h_{_Z} F_{_Z}(0)}{F_{_H}(0) + F_{_O}(0) + F_{_P}(0) + F_{_Z}(0)} \tag{C.15}$$

Param	Value	Units	Description
$r_{_H}$	1.6	yr^{-1}	Intrinsic growth rate for herbivorous fish
$r_{_O}$	1.3	yr^{-1}	Intrinsic growth rate for omnivorous fish
$r_{_P}$	1	yr^{-1}	Intrinsic growth rate for piscivorous fish
$r_{_Z}$	0.7	yr^{-1}	Intrinsic growth rate for top predator fish
$h_{_H}$	0.15	yr^{-1}	Harvesting rate for herbivorous fish
$h_{_O}$	0.15	yr^{-1}	Harvesting rate for omnivorous fish
$h_{_P}$	0.15	yr^{-1}	Harvesting rate for piscivorous fish
$h_{_Z}$	0.15	yr^{-1}	Harvesting rate for top predator fish
$m_{_H}$	0.1	yr^{-1}	Mortality due to predation for herbivorous fish
$m_{_O}$	0.1	yr^{-1}	Mortality due to predation for omnivorous fish
$m_{_P}$	0.1	yr^{-1}	Mortality due to predation for piscivorous fish
$\delta_{_O}$	0.5 ± 0.05	Unitless	Percentage of omnivorous fish diet consisting of algae
$\delta_{_P}$	0.4 ± 0.04	Unitless	Percentage of piscivorous fish diet consisting of herbivorous fish
$\delta_{_Z}^{H}$	0.1 ± 0.01	Unitless	Percentage of top predator fish diet consisting of herbivorous fish
$\delta_{_Z}^{O}$	0.3 ± 0.03	Unitless	Percentage of top predator fish diet consisting of omnivorous fish
$k_{_h}$	0 - 1	Unitless	Relative importance of local fish availability on harvesting rates
ν	0 - 1	Unitless	Dependence of harvesting on population growth

Table B.1: Parameters related to fish vital processes used in this paper. Mortality rates are assumed based on [25], $k_{_h}$ and ν are allowed to vary over broad potential ranges, and all other parameters are chosen to represent realistic biological scenarios.

Param	Value	Units	Description	Reference
q_b	0.0013 - 0.2	mg cm^{-3}	Baseline sediment concentration in rivers due to erosion	[28]
q_c	0.043, 0.31	mg cm^{-3}	Additional river sediment concentration when land is 100% cleared	[6, 7]
λ	1	yr^{-1}	Rate at which sediment in rivers is exported to reefs	Assumed
e	0.1 - 0.5 - 0.9	yr^{-1}	Rate at which suspended sediment on reefs leaves the system	[8]
k_{Dep}	4400	$100 \times$ cm yr^{-1}	Constant governing sediment deposition from water column to seabed	[31, 29]
κ_r	365	$100 \times$ mg cm^{-2} yr^{-1}	Sedimentation rate at which coral lateral growth is halved	[10]
κ_b	29.2	$100 \times$ mg cm^{-2} yr^{-1}	Sedimentation rate at which brooding coral recruitment is halved	[10]
κ_s	29.2	$100 \times$ mg cm^{-2} yr^{-1}	Sedimentation rate at which spawning coral recruitment is halved	[10]
κ_d	47.5	$100 \times$ mg cm^{-2} yr^{-1}	Sedimentation rate at which coral death is doubled	[10]
$\tilde{\phi}$	60	mg^{-1} cm^3	Constant relating non-algal food availability for omnivorous fish and sediment concentration	[18]
r_X	0 - 0.23 - 0.25	yr^{-1}	Deforestation rate	[32, 33]
a_X	0.18×0.23	yr^{-1}	Forest regrowth rate	[34]

Table B.2: Parameters related to sedimentation used in this paper.

Variable	Initial value
C	0.5457
T	0.2791
M	0.01
F_{H}	0.5165
F_{O}	0.7069
F_{P}	0.6554
F_{Z}	0.6738
S_{W}	0.0026
X	1

Table B.3: Initial conditions for each state variable in the model.

We then defined a harvesting rate for each functional group based solely on the relative availability of fish in that functional group as follows:

$$h_{\mathrm{Var},I}(t) = \frac{F_{I} h_{\mathrm{Tot}}}{F_{H}+F_{O}+F_{P}+F_{Z}}, \quad I \in \{H, O, P, Z\} \tag{C.16}$$

Since some fish species with high abundance (e.g. wrasses) are not expected to be of any commercial interest [35], we did not assume that the actual harvesting rates for each functional group would be solely based on relative fish abundances. Instead, we formulated harvesting rates $\bar{h}_{H}$, $\bar{h}_{O}$, $\bar{h}_{P}$, and $\bar{h}_{Z}$ for each functional group that would partly depend on the fishing rates parametrized from FishBase (i.e. the intrinsic demand for each functional group) and partially due to local fish availability. In other words, for a constant k_{h} representing the how important current local conditions are in determining demand for each functional group, we defined each $\bar{h}$ as follows:

$$\bar{h}_{I}(t) = \frac{h_{I}+k_{h} h_{\mathrm{Var},I}}{1+k_{h}}, \quad I \in \{H, O, P, Z\} \tag{C.17}$$

We also derived harvesting rates corresponding to constant fishing quotas for each fish functional group. To do this, we assumed that over a unit of time, the total number of fish harvested during that time would always be equal to a value $\rho \times \xi$, where ξ is the number harvested at time $t = 0$ and ρ is a scaling constant. ξ is defined below:

$$\xi = h_{H} F_{H}(0) + h_{O} F_{O}(0) + h_{P} F_{P}(0) + h_{Z} F_{Z}(0) \tag{C.18}$$

We further assumed that the different fish functional groups were harvested according to their proportions of the population. This means that, for ω a factor to ensure that the total fish harvested remains constant, the number of fish harvested in each functional group I is as follows:

$$\left(\frac{F_I}{F_H + F_O + F_P + F_Z}\right)\omega F_I \tag{C.19}$$

In order to obtain ω, we first noted that the number of fish harvested at each time step always being equal to $\rho \times \xi$ implies the following:

$$\sum_I \left(\frac{F_I}{F_H + F_O + F_P + F_Z}\right)\omega F_I = \rho\xi \tag{C.20}$$

By factoring out and isolating ω, we get the following:

$$\omega = \rho\xi\left(\frac{F_H + F_O + F_P + F_Z}{{F_H}^2 + {F_O}^2 + {F_P}^2 + {F_Z}^2}\right) \tag{C.21}$$

The harvesting rate for each functional group I is the number of fish harvested in that functional group divided by its total population. If we denote the harvesting rate as $h^a_{\mathrm{Var},I}$, with the a denoting that the amount harvested is what remains constant, we get the following:

$$h^a_{\mathrm{Var},I} = \frac{\omega F_I}{F_H + F_O + F_P + F_Z} = \frac{\rho\xi F_I}{{F_H}^2 + {F_O}^2 + {F_P}^2 + {F_Z}^2} \tag{C.22}$$

We noted that the denominator of this expression would get very close to zero if all fish species were nearing local extirpation, which was a likely scenario if fishing quotas remained constant. To avoid numerical errors in such a case, we used a modified version of Equation C.17, substituting $h^a_{\mathrm{Var},I}$ in place of $h_{\mathrm{Var},I}$ and taking $k_h = 999$. This gave us variable harvesting rates for each functional group that summed to a generally constant value:

$$\bar{h}_I(t) = \tfrac{1}{1000}\left(h_I + 999h^a_{\mathrm{Var},I}\right), \quad I \in \{H, O, P, Z\} \tag{C.23}$$

As we anticipated that constant harvesting amounts could cause the fish to go extinct, we additionally imposed the constraint while running the model that if the population of a functional group was below 10^{-6}, it would be treated as 0. This constraint further implied that the amount of fish harvested in such cases would also be zero. Calculation of fish extinction time was specifically done for herbivorous fish; since fish functional groups were harvested in this case according to their proportions of the total fish population, all functional groups that went extinct did so at the same time. (This put the threshold for local extinction of all fish functional groups combined at 4×10^{-6}.)

D Dependence of fish resilience to deforestation-induced sedimentation on local hydrological conditions

To determine how the changes brought about by deforestation depend on local conditions, we ran simulations of highland deforestation with q_b (the baseline sediment concentration in local rivers) and e (the rate at which sediment is flushed out of the system) varying within their entire ranges. Here, we took $r_X = 0.23$. Initial conditions for fish were taken to be their theoretical population

maxima (i.e. 1 for each functional group); all other initial conditions were taken to be their steady-state values when no deforestation takes place and all parameters are at their baseline values. This was done in order to isolate the transient dynamics produced by different local conditions for the same amount of deforestation pressure. In each simulation, we obtained the population of each fish functional group at $t = 20$.

We found that the effects of baseline local conditions on resilience of reef fish to deforestation-driven sedimentation was heterogeneous across functional groups. Taking the population levels of each fish functional group following 20 years of heavy deforestation on steep slopes ($r_x = 0.23$, $q_c = 0.31$) revealed the expected patterns of fish resilience being greater for higher values of e and lower values of q_b. As was the case when we examined changes in fish populations as a function of deforestation rate (Figure 2 in the main manuscript), we found that more turbid starting conditions (lower e and higher q_b) affected omnivorous fish the most, whereas herbivorous fish had the broadest range of conditions under which they were able to maintain at least a moderate population size (Figure D.2). We additionally found that the dependence of fish populations following deforestation on baseline river sediment concentration q_b was sigmoidal, with large changes in fish population levels around 1×10^{-2} mg cm^{-3} for most functional groups, and at somewhat greater concentrations for herbivorous fish.

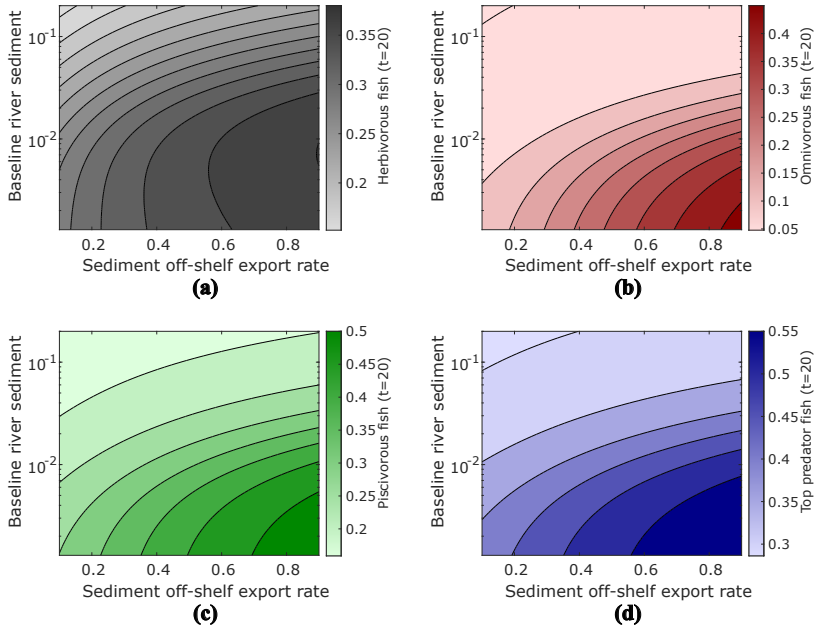

Figure D.2: Population levels of herbivorous fish (Figure D.2a), omnivorous fish (Figure D.2b), piscivorous fish (Figure D.2c), and top predator fish (Figure D.2d) after 20 years of highland logging, showing dependence on baseline sediment levels from erosion q_b and off-shelf sediment export rate e. Initial conditions for fish functional groups were taken to be that functional group's theoretical maximum population (i.e. 1) in all cases.

References

[1] C. H. R. Goatley, D. R. Bellwood, Sediment suppresses herbivory across a coral reef depth gradient, Biology Letters 8 (6) (2012) 1016–1018. doi:10.1098/rsbl.2012.0770.

[2] S. B. Tebbett, C. H. Goatley, R. P. Streit, D. R. Bellwood, Algal turf sediments limit the spatial extent of function delivery on coral reefs, Science of The Total Environment 734 (2020) 139422. doi:10.1016/j.scitotenv.2020.139422.

[3] R. Froese, D. Pauly, Fishbase, www.fishbase.org (2022).

[4] S. Tanaka, R. Nishii, A model of deforestation by human population interactions, Environmental and Ecological Statistics 4 (1) (1997) 83–92. doi:10.1023/a:1018510125512.

[5] United Nations, Department of Economic and Social Affairs, Population Division, World population prospects 2019: Online edition (2019).
URL https://population.un.org/wpp/Download/

[6] D. T. Neil, A. R. Orpin, P. V. Ridd, B. Yu, Sediment yield and impacts from river catchments to the Great Barrier Reef lagoon: a review, Marine and Freshwater Research 53 (4) (2002) 733. doi:10.1071/mf00151.

[7] A. S. Wenger, S. Atkinson, T. Santini, K. Falinski, N. Hutley, S. Albert, N. Horning, J. E. M. Watson, P. J. Mumby, S. D. Jupiter, Predicting the impact of logging activities on soil erosion and water quality in steep, forested tropical islands, Environmental Research Letters 13 (4) (2018) 044035. doi:10.1088/1748-9326/aab9eb.

[8] J. Walsh, C. Nittrouer, Contrasting styles of off-shelf sediment accumulation in New Guinea, Marine Geology 196 (3-4) (2003) 105–125. doi:10.1016/s0025-3227(03)00069-0.

[9] B. Ferré, X. D. de Madron, C. Estournel, C. Ulses, G. L. Corre, Impact of natural (waves and currents) and anthropogenic (trawl) resuspension on the export of particulate matter to the open ocean, Continental Shelf Research 28 (15) (2008) 2071–2091. doi:10.1016/j.csr.2008.02.002.

[10] T. Fung, R. M. Seymour, C. R. Johnson, Alternative stable states and phase shifts in coral reefs under anthropogenic stress, Ecology 92 (4) (2011) 967–982. doi:10.1890/10-0378.1.

[11] A. S. Hoey, D. R. Bellwood, Cross-shelf variation in the role of parrotfishes on the Great Barrier Reef, Coral Reefs 27 (1) (2007) 37–47. doi:10.1007/s00338-007-0287-x.

[12] F. X. Latrille, S. B. Tebbett, D. R. Bellwood, Quantifying sediment dynamics on an inshore coral reef: Putting algal turfs in perspective, Marine Pollution Bulletin 141 (2019) 404–415. doi:10.1016/j.marpolbul.2019.02.071.

[13] Y. Akita, T. Kurihara, M. Uehara, T. Shiwa, K. Iwai, Impacts of overfishing and sedimentation on the feeding behavior and ecological function of herbivorous fishes in coral reefs, Marine Ecology Progress Series 686 (2022) 141–157. doi:10.3354/meps13996.

[14] K. E. Havens, J. R. Beaver, D. A. Casamatta, T. L. East, R. T. James, P. Mccormick, E. J. Phlips, A. J. Rodusky, Hurricane effects on the planktonic food web of a large subtropical lake, Journal of Plankton Research 33 (7) (2011) 1081–1094. doi:10.1093/plankt/fbr002.

[15] A. L. Downing, B. L. Brown, E. M. Perrin, T. H. Keitt, M. A. Leibold, Environmental fluctuations induce scale-dependent compensation and increase stability in plankton ecosystems, Ecology 89 (11) (2008) 3204–3214. doi:10.1890/07-1652.1.

[16] Y. Tao, S. A. Campbell, F. J. Poulin, Dynamics of a diffusive nutrient-phytoplankton-zooplankton model with spatio-temporal delay, SIAM Journal on Applied Mathematics 81 (6) (2021) 2405–2432.

[17] C. M. Heggerud, H. Wang, M. A. Lewis, Transient dynamics of a stoichiometric cyanobacteria model via multiple-scale analysis, SIAM Journal on Applied Mathematics 80 (3) (2020) 1223–1246. doi:10.1137/19m1251217.

[18] J. E. Cloern, Turbidity as a control on phytoplankton biomass and productivity in estuaries, Continental Shelf Research 7 (11-12) (1987) 1367–1381. doi:10.1016/0278-4343(87)90042-2.

[19] M. M. Nugues, C. M. Roberts, Coral mortality and interaction with algae in relation to sedimentation, Coral Reefs 22 (4) (2003) 507–516. doi:10.1007/s00338-003-0338-x.

[20] D. R. Bellwood, C. J. Fulton, Sediment-mediated suppression of herbivory on coral reefs: Decreasing resilience to rising sea-levels and climate change?, Limnology and Oceanography 53 (6) (2008) 2695–2701. doi:10.4319/lo.2008.53.6.2695.

[21] A. Wakwella, P. J. Mumby, G. Roff, Sedimentation and overfishing drive changes in early succession and coral recruitment, Proceedings of the Royal Society B: Biological Sciences 287 (1941) (2020) 20202575. doi:10.1098/rspb.2020.2575.

[22] S. J. Thackeray, T. H. Sparks, M. Frederiksen, S. Burthe, P. J. Bacon, J. R. Bell, M. S. Botham, T. M. Brereton, P. W. Bright, L. Carvalho, et al., Trophic level asynchrony in rates of phenological change for marine, freshwater and terrestrial environments, Global Change Biology 16 (12) (2010) 3304–3313.

[23] D. Souter, S. Planes, J. Wicquart, M. Logan, D. Obura, F. Staub (Eds.), Status of Coral Reefs of the World: 2020, Global Coral Reef Monitoring Network, 2020.

[24] J. A. Dunne, R. J. Williams, N. D. Martinez, Network structure and robustness of marine food webs, Marine Ecology Progress Series 273 (2004) 291–302.

[25] J. C. Blackwood, A. Hastings, P. J. Mumby, A model-based approach to determine the long-term effects of multiple interacting stressors on coral reefs, Ecological Applications 21 (7) (2011) 2722–2733. doi:10.1890/10-2195.1.

[26] V. A. Thampi, M. Anand, C. T. Bauch, Socio-ecological dynamics of Caribbean coral reef ecosystems and conservation opinion propagation, Scientific Reports 8 (1) (2018). doi:10.1038/s41598-018-20341-0.

[27] P. Dalzell, Catch rates, selectivity and yields of reef fishing, in: Reef Fisheries, Springer Netherlands, 1996, pp. 161–192. doi:10.1007/978-94-015-8779-2_7.

[28] N. Hutley, M. Boselalu, A. Wenger, A. Grinham, B. Gibbes, S. Albert, Evaluating the effect of data-richness and model complexity in the prediction of coastal sediment loading in Solomon Islands, Environmental Research Letters 15 (12) (2020) 124044. doi:10.1088/1748-9326/abc8ba.

[29] S. Albert, P. L. Fisher, B. Gibbes, A. Grinham, Corals persisting in naturally turbid waters adjacent to a pristine catchment in Solomon Islands, Marine Pollution Bulletin 94 (1-2) (2015) 299–306. doi:10.1016/j.marpolbul.2015.01.031.

[30] R. Bartley, Z. T. Bainbridge, S. E. Lewis, F. J. Kroon, S. N. Wilkinson, J. E. Brodie, D. M. Silburn, Relating sediment impacts on coral reefs to watershed sources, processes and management: A review, Science of The Total Environment 468-469 (2014) 1138–1153. doi:10.1016/j.scitotenv.2013.09.030.

[31] H. Rügner, M. Schwientek, B. Beckingham, B. Kuch, P. Grathwohl, Turbidity as a proxy for total suspended solids (TSS) and particle facilitated pollutant transport in catchments, Environmental Earth Sciences 69 (2) (2013) 373–380. doi:10.1007/s12665-013-2307-1.

[32] D. L. A. Gaveau, D. Sheil, Husnayaen, M. A. Salim, S. Arjasakusuma, M. Ancrenaz, P. Pacheco, E. Meijaard, Rapid conversions and avoided deforestation: examining four decades of industrial plantation expansion in Borneo, Scientific Reports 6 (1) (2016). doi:10.1038/srep32017.

[33] Statistics Indonesia, Penduduk Indonesia menurut provinsi 1971, 1980, 1990, 1995, 2000 dan 2010, in Indonesian (Dec. 2021).
URL https://bps.go.id/statictable/2009/02/20/1267/penduduk-indonesia-menurut-provinsi-1971-1980
html

[34] C. Vancutsem, F. Achard, J.-F. Pekel, G. Vieilledent, S. Carboni, D. Simonetti, J. Gallego, L. E. O. C. Aragão, R. Nasi, Long-term (1990–2019) monitoring of forest cover changes in the humid tropics, Science Advances 7 (10) (2021). doi:10.1126/sciadv.abe1603.

[35] T. R. McClanahan, R. Arthur, The effect of marine reserves and habitat on populations of East African coral reef fishes, Ecological Applications 11 (2) (2001) 559–569. doi:10.1890/1051-0761(2001)011[0559:teomra]2.0.co;2.